Effects of Pine Rosin on the Degradation of Mechanical Performance in Flax-Reinforced Polymeric Composites after Soil Burial at Low Temperatures

Lauri Jutila,[a] Rama Layek,[b] Farzin Javanshour,[a] Lijo George,[a] Essi Sarlin,[a] and Mikko Kanerva [a,*]

The effect of pine rosin (RO) was studied relative to the biodegradation of poly(lactic acid) (PLA), starch-based polymer (Mater-Bi), and PLA-flax composites. It was hypothesized that rosin can alter – either speed up or slow down – biodegradation in plastics depending on the specific species of polymer. The biodegradation was brought about by soil burial over 56 days. First, the effect of rosin was studied alone without any effects of soil burial. Second, the effects of soil burial were studied in terms of biodegradation. The results showed that RO increased the degree of crystallinity (+100%) and Young's modulus (+14%) of PLA. For Mater-Bi, RO decreased the strength by 22% and led to brittleness (56% lower ultimate strain) of the specimens. After 56 days of soil burial, the presence of RO in PLA was found to speed up the degradation when compared to pure PLA (the decrease of strength was 9.3% and 6.6%, respectively). For Mater-Bi, the RO blending led to 2.1% slower biodegradation of strength during 56 days of soil burial. The effect of RO, in terms of affecting the biodegradation, was comparable in flax-reinforced and non-reinforced PLA. The strength of the fiber-matrix bonding remained equal for RO-impregnated fibers compared to the as-received flax fibers.

DOI: 10.15376/biores.18.1.899-925

Keywords: Composite; Flax; Rosin; Soil burial; Interface

*Contact information: a: Unit of Materials Science and Environmental Engineering, Tampere University, P. O. Box 589, Tampere, FI-33720 Tampere, Finland; b: LUT University, Department of Separation Science, FI-15210 Lahti, Finland; *Corresponding author: mikko.kanerva@tuni.fi*

INTRODUCTION

Structural components have requirements of stiffness, strength, and durability. The requirement of durability is controversial regarding the needs of developing degradable or compostable parts. Biological degradation and recycling of polymeric materials are the two necessary routes to make these materials sustainable. The barriers in the implementation of sustainable strategies are related to the lack of knowledge and time constraints within industrial material development (Veshagh *et al.* 2012). The recycling of fiber-reinforced composite materials often leads to heavy down-cycling (Yazdanbakhsh and Bank 2014; Oliveux *et al.* 2015). Moreover, biodegradable composites lack mechanical performance, such as strength and toughness, compared with the high-performance composites with rival matrix polymers and fibers of carbon, aramid, and glass (Kumar and Kumar 2012). Natural fiber composites are increasingly intended for novel applications (Hoffmann *et al.* 2021; Graupner *et al.* 2022). For the transmission line poles of data networks (Di Vito *et al.* 2020), large amounts of poles would be placed in rural areas. The protection covers, as

well as enclosure parts of the poles may experience failure due to lack of mechanical performance in the harsh environment of the application.

There is clearly a need to adjust the long-term performance of biodegrading composite materials. For these composites, there should be no toxic or non-degradable (synthetic) chemicals added unless their time-wise reactions in the material system would finally make them degradable and non-toxic. The biodegradation rate of materials, in general, is a function of prevailing micro-organisms, oxygen and water content, temperature, pH, and electrolytes (Müller 2014; Crawford *et al.* 2017). The polymeric structure must contain suitable chemical groups, including esters that react with natural organisms and enzymes.

There have been many studies in which decomposition reactions have been shown to be affected by additives. Pro-oxidants such as Mn/Fe and Mn metal salts increase the biodegradability of polypropylene (Fontanella *et al.* 2013). Likewise, polystyrene biodegrades in the case of formation of carbonyl groups to its structure (Ojeda *et al.* 2009). For fibrous composites, the biodegradation of flax fiber-reinforced polylactic acid (PLA) can be improved with additives, such as amphiphilic compounds (Kumar *et al.* 2010). Alternatively, biodegradation can be hindered with dicumyl peroxide (Kumar *et al.* 2010). It should be noted that there are indigenous fungal species inside flax fibers, due to dew-retting, and they tend to affect the biodegradation rate (Crawford *et al.* 2017). Traditionally, biostabilization is achieved using biocides (Falkiewicz-Dulik *et al.* 2015); biocides are divided into four different main groups, *i.e.*, disinfectants and general biocidal products, preservatives, pest control, and other biocidal products. Most of the biocides are harmful or toxic to several living species. For composting polymer composites (Endres and Sieber-Raths 2011), especially during aerobic processes (Rudnik 2008), the formed compost should be directly usable as fertilizer, manufactured topsoil, mulch, and growing medium in agriculture. Therefore, all the materials and additives in the materials composted should be non-toxic, or the toxic components should completely decompose during the composting process.

In nature, extractive components in plants affect decomposition. In pine tree trunks (*e.g.*, *Pinus pinaster* and *P. sylvestris*), rosin prevents decomposition by molds and fungi in the core of the trunk, *i.e.*, the heartwood (Himejima *et al.* 1992; Sjöström 1993; Ekeberg *et al.* 2006). In other parts of the trunk (in the sapwood), rosin has similar functions, yet with a modified chemical composition, due to its other roles, such as being a nutrition carrier. In living trees, rosin may leak from the tree bark and is further taken advantage of by insects, such as ants. Rosin works as a disinfector for ants and inhibits the growth of mold and fungi inside their nests (Chapuisat *et al.* 2007). Rosin has long been used by humans, who blend it with synthetic materials. Rosin acts against health-endangering organisms (Söderberg *et al.* 1990; Vainio-Kaila *et al.* 2017a; Niu *et al.* 2018; Abdel-Raouf and Abdul-Raheim 2018); it is used as an anti-microbial additive in medicine and medical products.

This study analyzed the effects of pine rosin when it is blended into plastics. Also, its use in flax-reinforced composites, and rosin's effect on the biodegradation related to soil burial were studied. The most recent results (Hakala *et al.* 2022) for this type of natural fiber-reinforced composites indicated remarkable effects of soil burial in terms of flexural performance, yet it indicated an unclear influence of rosin. To understand flexural performance in detail, the in-plane behavior must be studied. In order to resolve the changes in isotropic matrix polymers, the current work studied injection-molded samples in the first phase. Two degradable polymer matrices were studied, namely PLA and a

starch-based compound Mater-Bi, in addition to epoxy as a reference. In the second phase of the study, different rosin integration techniques, namely blending and fiber impregnation, were studied in composites exposed to soil burial. In the results and analysis, the effects of rosin on the degradation routes of biotic and abiotic degradation, moisture diffusion, and interfacial adhesion were considered.

EXPERIMENTAL

Pine Rosin

Pine rosin (specifically gum rosin) was provided by Forchem (Rauma, Finland): batch ww-16032017 with an acid value of 167 mg KOH/g. This rosin batch had a softening point of 74 °C and the onset of thermal degradation at 200 to 220 °C; more details about the behavior of this rosin batch can be found in recent works (Kanerva *et al.* 2019; Kanerva *et al.* 2020). Rosin (RO) was received in the form of solid crushed particles with a proper size for compounding. The chemical content of RO was analyzed by a mass spectrometer (JMS-T100LP AccuTOF 4G, JEOL, Tokyo, Japan) equipped with the DART ionization source (IonSense Inc., Saugus, MA, USA). The spectra were processed to centroid; calibration and drift correction with polyethylene glycol 600 were applied. In addition, the proton nuclear magnetic resonance (NMR) spectrum was recorded at 500 MHz by using the ECZR 500 MHz NMR spectrometer (JEOL). In this study, the chemical shifts (δ) are reported in parts per million (ppm) referenced to the TMS peak (δ 0.00). For NMR, rosin was dissolved in deuterated chloroform.

Matrix Polymers

Poly(lactic acid) (PLA) (Ingeo 2003 D) was provided by NatureWorks (Minnetonka, MN, USA). This PLA is one of the most typical 'biopolymers' because it originates from renewable resources, and it can degrade under the conditions of industrial composting. This grade has nominally less than 0.3% of residual lactide according to the manufacturer; the D-lactide content has been reported to be ≈2.5% for the 2000-series (2002 D) (Puchalski *et al.* 2017). In this study, PLA was compounded at 200 °C with RO by using a twin-screw extruder (TSE 25E, Brabender, Duisburg, Germany). For the mixing, RO particles were fed to the hopper simultaneously with PLA granulate. RO was fed directly through the hopper of a compounder. Additionally, a batch of pure PLA was compounded (*i.e.*, run through the extruder) to form a series with similar processing effects (on PLA) than for the series with blended RO. The granulated PLA and PLA-RO compounds were fed to an injection molding device (single-screw α-C30, Roboshot) to form standard (ASTM D 638-14) tensile dog-bone specimens (10 at a minimum per series); the parameters are specified in Table 1. Before the injection, PLA and PLA-RO granules were dried (at 60 °C overnight).

Table 1. Injection Parameters Used in this Work to Prepare Tensile Specimen

Matrix	Extruder (screw) Temperature (°C)	Hold Pressure (bar)	Hold Time (s)	Cooling Time (s)
PLA	220	700	10	30
PLA-RO	200	400	30	30
MBi	160	250	10	25
MBi-RO	160	190	15	30

In addition to PLA, a starch-based biopolymer product Mater-Bi (Novamont, Novara, Italy) was studied. Mater-Bi (denoted MBi in this work) is a system of compatibilized starch and polycaprolactone. Typically, MBi is applied in thin sheets (Bastioli 2002). Here, MBi was compounded with RO in a similar process as PLA but at 160 °C. A processed sample series without any RO was prepared for comparison. Granulated MBi and MBi-RO compounds were fed to the above-mentioned injection device to form standard (ASTM D 638-14) tensile dog-bone specimens, 10 at a minimum per series. The injection parameters are given in Table 1. Before the injection, MBi and MBi-RO granules were dried at 35 to 40 °C overnight, noting that MBi is unstable at higher drying temperatures.

Flax-Reinforced Composite Laminates

Flax-reinforced composite laminates were prepared by using 2×2 twill reinforcement of flax (200 g/m^2, Biotex, Chesterfield, UK) with an epoxy thermoset resin (Super Sap CLR, Entropy Resins, Hayward, CA, USA) *via* vacuum-assisted resin-infusion. The laminates had a stacking sequence of $[0/45]_{SE}$, and the reinforcement was dried before infusion to remove moisture carefully (at 80 °C, for 1 h, following a dwell at 100 °C, for 1 h). The infusion took place on a glass surface and a vacuum bag (vacuum pressure difference 0.5 bar) was used to form the laminates. The solid laminates were post-cured in an oven (at 80 °C, for 2 h).

Thermoplastic composite laminates were prepared by combining the flax reinforcement (layer by layer) and PLA and PLA-RO in a hot press. PLA with and without rosin was used in a granulated form; pure PLA had been compounded to ensure a comparative amount of processing-induced damage on PLA. First, PLA and PLA-RO plates were prepared by the press (at 180 °C, 100 bar, for 10 min). A metal frame was used to confine polymer at an exact volume. Second, the reinforcement and PLA layers were formed and finally stacked to form laminates (into the lay-up $[0/45]_{SE}$) and consolidated (at 180 °C, 100 bar, for 5 ± 1 min for single layer and 8 ± 0.1 min for laminates). When using PLA-RO granules, the pressing temperature was lowered to 160 °C. The flax reinforcement was dried before the pressing (at 90 °C, for 2 h).

In addition to the above laminate series, a rosin-impregnated series (PLA-F-Imp) was prepared. For this method of RO usage, the dried flax reinforcement was immersed in a rosin-ethanol solution (10 m-% of rosin) for 24 h and dried at the ambient room temperature. After the impregnated reinforcement pieces had been dried, the laminates with PLA-RO matrix were prepared *via* hot pressing.

Single Filament-Matrix Samples for Microbond Testing

A rosin-ethanol solution (10 m-% of rosin) was mixed to form a bath for coating of single filaments. Flax filaments were treated for 10 min by immersion to the solution and lastly, rinsed in ethanol. PLA droplets were deposited onto the filaments at 185 °C under a nitrogen atmosphere to minimize oxidation of the small droplets.

Soil Burial

The soil burial (SB) conditioning was carried out in half-warm (not technically controlled) indoor premises (10.6 ± 1.9 °C, 62 ± 8% RH) using a commercial compost bin Biolan 220eco (Biolan, Eura, Finland). During the SB, temperature was digitally monitored and constantly recorded (175H1 & 175T2, Testo, Titisee-Neustadt, Germany) in three

locations of the bin and also manually observed with an analogue meter integrated into the middle of the bin. In addition, relative humidity was digitally recorded at two points amid the bin. For details, see Fig. 1. Here it was opted, due to the non-specific procedure, to have all the specimens conditioned at once, to ensure comparable effect due to the SB. The different specimen series were separated by inert stainless steel (AISI 304) mesh into four sections so that any release of rosin (from specimens) would not get transferred towards the non-rosin test specimens (by gravity or capillary flow) and to allow removal of specimens at two different time points (*i.e.*, 14 and 56 days). The specimens from each series were buried essentially in a similar way in different depths of the bin because the top and bottom of the bin experience different moisture content and temperature; thus, the potential for different rates of microbial processes. This means that the deviations in mechanical testing results will engulf the variation inside the bin, but the experimental scatter between different series is anticipated to be similar (to allow for comparison of average strength values).

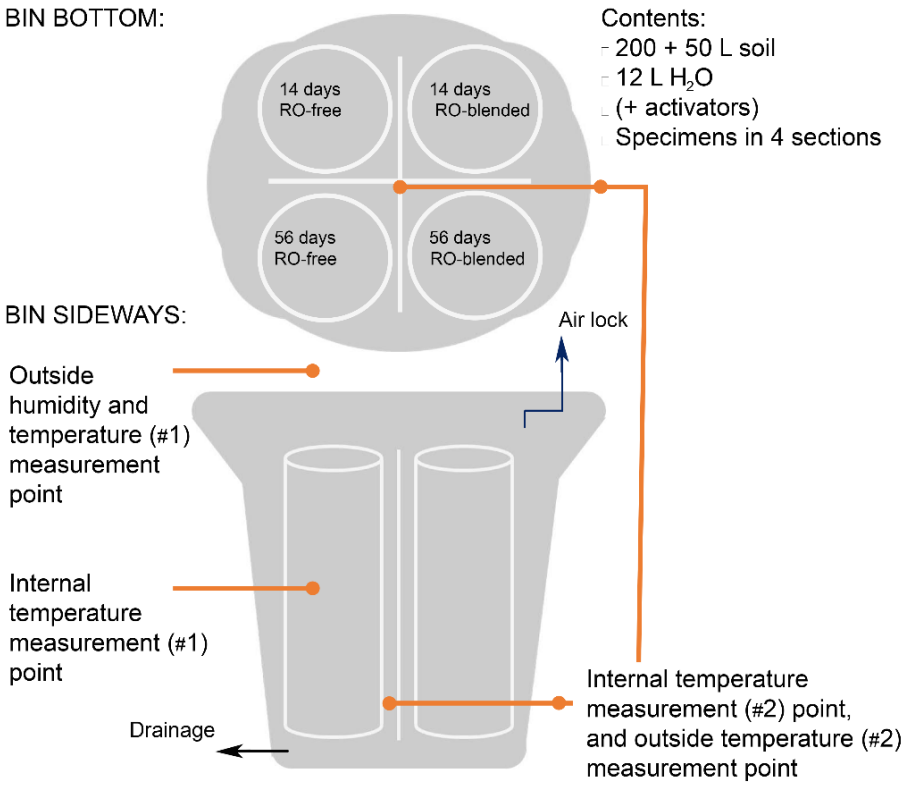

Fig. 1. The compost bin and specimen arrangement in four sections during SB in this study.

The soil used for SB was a mixture (ratio of 200/50) of commercial garden peat (N 15 mg/L, P 100 mg/L, K 500 mg/L) (Biolan) and forest surface soil (humus, leaves, small branches) typical of Scandinavia (site location ≈61.483 N) to imitate household composting or natural decomposition. Within the loading of the bin, external moisture by 12 L of water (≈37 °C) was gradually included so that the final added moisture ratio of 4.8% (volume/volume) was reached during the conditioning. For part of the water added in the beginning, two different compost activators (Neko, Hämeenlinna Finland; Multikraft Produktions und Handels, Pichl bei Wels, Austria) were used (the microbial and enzymatic contents are tabulated in the Appendix section). Microbial coverage (mold, fungi) on the

specimens were typically observed right after the removal from the bin. The temperature profiles during SB are shown in Fig. 2. The composting process achieved the peak temperature (16.2 °C, compared to the temperature of the surroundings 10.6 ± 1.9 °C) within ≈8 days and then slowly cooled down towards the average temperature of the surroundings. The low peak temperature is due to the low nutrient content of the soil mixture in the mesophilic (Rudnik 2008) phase.

After 14 days of SB, the mass changes in the specimens were negligible (within measurement accuracy). After 56 days, mass changes were 0.3 to 4.7% (see more in the Results section), except for the epoxy-series composites where clearly a lower mass gain range was observed (<1.2%). As a rough literature reference, starch-blended polymers (*e.g.*, blends with polyhydroxyalkanoates) in thin film form totally disintegrate in around 150 days in tropical conditions (Müller 2014). For PLA, SB in ≈25 °C have been reported to result in 5 to 25% mass loss in 50-90 days when PLA is blended with amphiphilic additives (Kumar *et al.* 2010).

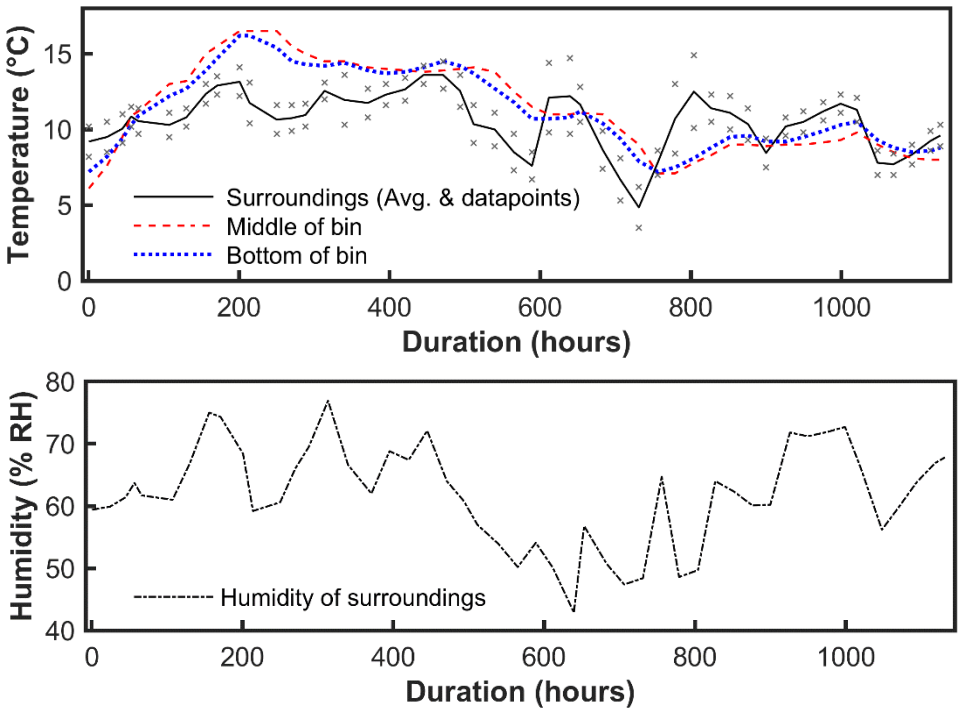

Fig. 2. Internal and outside temperatures (see the exact sensor points in Fig. 1), and the recorded outside (surroundings) relative humidity during the SB conditioning.

Tensile Testing

Tensile testing was carried out by using a universal tester (model 5967, Instron, Norwood, MA, USA) with a 30 kN load cell. Tensile test specimens according to the standard (ASTM D 638-14) were tested with a dog-bone shape for the test series of injected matrix polymers. For the composites, rectangular-shaped specimens were used with the dimensions 250 mm × 10 mm × 1 mm (length × width × thickness). For maximum accuracy, the tensile strain was measured by using an auxiliary extensometer (50 mm gauge length). For PLA and PLA-RO as well as MBi and MBi-RO series, the extensometer was removed after reaching 1% of strain (or 2 mm displacement) due to the anticipated rubbery behavior beyond the allowed extensometer operation. In addition to force, strain, and

displacement data, individual thickness and width were measured per specimen both prior to and after testing. Whenever the amount of necking at the failure point was noticeable within the measurement accuracy, true stress (and logarithmic strain) values were calculated for the ultimate failure and over the test range as is reasonable for very high absolute values of strain. The specimens were dried after SB, before testing, to exclude the plasticizing effect of moisture (and when compared to reference specimens in ambient conditions); the recorded dehydration profiles of the specimens are published elsewhere (Jutila 2020).

Young's moduli were determined based on (elastic) stress and extensometer-given strain data by using least-squares fitting for linear regression. Primarily, strain data below 0.5% was used. A decrease in the data range (to 0.25%) was used to decrease the regression error for the rosin-impregnation series (PLA-F-Imp). The lower bound of strain in fitting was determined per test series to exclude initial non-linearity (*e.g.*, due to slight specimen bending). In addition to Young's moduli, ultimate (engineering) stress and strain values were collected to analyze final failure. Average values and standard deviations were calculated per series.

Microbond Testing of Interfaces

The apparent interfacial shear strength (IFSS) between flax fiber and PLA was studied with the microbond technique to analyze the changes in adhesion due to rosin. For the test specimen preparation, elementary flax fibers were extracted from flax fabrics by tweezers under an optical microscope and fixed on a stainless-steel sample holder with epoxy glue. The average diameter of elementary flax fibers was 15 ± 3 μm. For surface modification with rosin, fibers were dipped into a 10 m-% rosin-ethanol solution for 10 minutes and rinsed three times in ethanol to remove loose and excessive rosin coating. Both PLA granules and flax fibers were stored in the oven at 60 °C for 24 h before droplet deposition. PLA droplets of different sizes were deposited on flax fibers with FIBRODrop (Fibrobotics Oy, Tampere, Finland) device based on the resin dip method. A fraction of PLA granulate was placed in an aluminum block with a cylindrical cavity. The PLA droplets were deposited at 185 °C, while the melt flow during droplet deposition was monitored with a computer-controlled embedded heating element. Droplets were deposited in an air-tight cabinet filled with nitrogen gas to prevent potential oxidation of the melting PLA. The average embedded length of the samples was 75 ± 17 μm (larger discarded to avoid fiber failure during the testing). Droplets that had a higher volume than the single flax fiber were selected for testing. The microbond measurements were performed with a FIBRObond (Fibrobotics, Finland) device (Laurikainen *et al.* 2020) with 1 N load cell and 0.008 mm/s loading rate. The diameter of the fibers and the embedded length of the droplets were captured before each measurement with an optical microscope (model UI-3370SE, IDS, Germany) of the FIBRObond device. During the test, microvices sheared the droplets until complete debonding. Here, the microvices were standard (medical) blades. The slope of the linear regression of maximum debonding force of individual droplets *vs.* embedded area was considered to be the apparent IFSS. In total, 50 individual droplets were tested for each of the unmodified and rosin-modified elementary flax fibers.

Polymer Characterization and Fracture Imaging

X-ray diffraction (XRD) was used to analyze the crystallinity of the laminates with PLA before and after the SB conditioning. It was hypothesized that SB could essentially affect crystallinity in PLA. Empyrean Multipurpose (Malvern Panalytical, Malvern, UK)

diffractometer with copper K_α radiation (λ = 1.5406 cm^{-1}), and steps of 0.013° were used.

The crystallinity in PLA was further studied using differential scanning calorimetry (DSC) by using a DSC 214 device (Netzsch, Bayern, Germany). The measurements were run at nitrogen atmosphere (40 to 60 mL/min) and the heating ramp was linear (10 °C/min) over the temperature range of -20 to 200 °C. Sample pans were sealed with a pierced aluminum lid. Two heating cycles were performed, but the first cycle was used in order to study the crystallinity of the sample (sample weight ≈5 to 7 mg) at the after-compost condition. From the data, the endothermic peak of melting (Δh_m) and the change of enthalpy due to (cold) crystallization (Δh_{cc}) were determined. Based on the literature about fully crystalline PLLA (Δh_{c100} = 93 J/g (Ray and Okamoto 2003)), the degree of crystallinity was calculated as $K = (\Delta h_m - \Delta h_{cc}) / \Delta h_{c100}$. Here, the tensile test specimens after 14 days of SB were used for the analysis because most of the degradation in PLA-based specimens occurred during the first 14 days (see the results in later sections).

For fractography, after tensile testing, the fracture surfaces of the laminates were studied with scanning electron microscopy, SEM (ULTRAplus, Zeiss, Oberkochen, Germany). The main target was to determine failure in detail at the fiber-polymer interfaces. The samples were coated with a thin gold layer to ensure the required conductivity.

RESULTS AND DISCUSSION

Rosin Acids

RO is a chemically complex substance that involves phenolic compounds, waxes, a large variety of fatty acids and terpenoid, sterol, and terpene acids. From the mass spectrometry results (see the spectrum in the Appendix section), abietic acid and its isomers were identified with an *m*/*z* value of 303.23236 $[M+H]^+$, dehydroabietic acid at 301.21691 $[M+H]^+$, and methyl ester of abietic acid at 317.21186 $[M+H]^+$. Naturally, the isomers could not be distinguished despite having been suggested previously by the results of volatile organic compounds analysis (Kanerva *et al.* 2021). The measured NMR spectrum (see spectrum and details in the Appendix section) in general matched the NMR spectra of rosin (or pine resin) reported in the literature (Skakovskii *et al.* 2008). Here, the presence of individual resin acids could be identified from the measured spectra by comparing it with the reported spectra, and this indicated the presence of pimaric, isopimaric, levopimaric, and palustric acid in the rosin batch of this study. The carboxylic acid group (−COOH) has been reported as a probable biodegradation-inducing factor (Hubbe *et al.* 2021) for PLA featuring crystalline phases.

Degradation of In-plane Stiffness and Strength

Mechanical performance of PLA and MBi without flax reinforcement

The stress-strain behavior of the matrix specimens and the reinforced composite specimens was nonlinear, as shown in Figs. 3 and 6. The PLA and MBi series experienced extensive plastic deformation independent of the RO content or SB duration as is expected for this type of base polymers. The flax-reinforced composites experienced either a smooth or bi-linear kind of behavior (see Fig. 6). The bi-linear behavior has been reported to indicate the start of visco-plastic deformation of the amorphous zones inside the different lamellar layers or S-walls of flax, a phenomenon that has been observed in the tests of elementary fibers as well (Giancane *et al.* 2010; Bensadoun *et al.* 2017). The computed

mechanical properties are presented in Tables 2 to 4.

RO alone is a mechanically weak and brittle solid at room temperature. Whenever there is no chemical modification of the base polymer by RO, the common rule of mixtures predicts lower strength and stiffness in any kind of mixture with PLA. For the reference condition (*i.e.*, Ref. curves in Figs. 3 and 6), the absolute effect of RO on Young's modulus was -7.5% when calculated over all the test series. Similarly, the effect of RO on the strength in the reference condition, when calculated over all the series, was -15.8%. To be precise, the peak engineering stress values differed from stress at break, especially for the MBi series. Thus, true stress-logarithmic strain curves are given in the Appendix section, and the visually observed necking at the final failure location can be seen in Fig. 4. However, specifically for PLA, the compounding with RO resulted in a higher Young's modulus: the Ref. modulus increased on average ≈14% (for pure polymer specimens: +13.6%, and for composites +10.4%). By noting that the linear regression for Young's modulus fitting was good ($R^2 > 0.994$) and the standard deviations were low or moderate (average COV 18%) over the PLA and PLA-RO series, the observed stiffening is suggested to be due to changes in crystallinity or changes in the PLA's chemistry upon compounding with rosin.

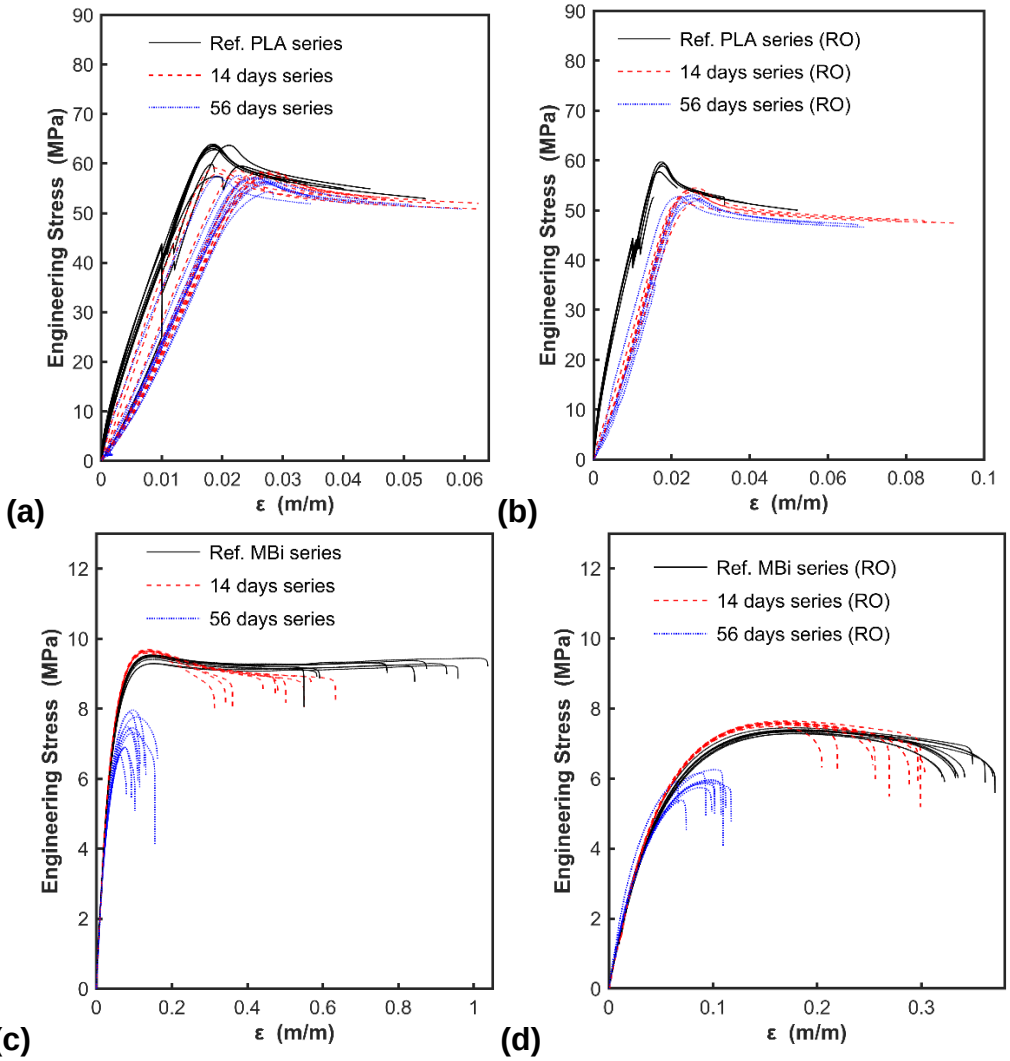

Fig. 3. Tensile stress-strain curves for solid matrix polymers in the reference state and after soil burial of 14 days and 56 days. The specimens were dried after soil burial before testing. RO

refers to rosin blending.

The MBi series lost a considerable part (-46%) of its stiffness due to RO blending. The strain at break also decreased (-56%), which indicates increased brittleness and decreased molecular weight. The −COOH groups of various acids of RO are anticipated to react with hydroxyl groups in starch-based content of MBi. This would result in moisture as a by-product of the reactions (Imre and Vilaplana 2020). In general, MBi is sensitive to moisture during processing but also during storage. The ester bonds in MBi may also undergo hydrolysis in the presence of weak RO acids. Additionally, the phase boundaries of polysaccharide and polycaprolactone have been suggested as weak points (Singh *et al.* 2003).

In terms of normalized effects per duration of SB, the effect due to RO would be 'to speed up' if there were a larger change in stiffness and strength with RO-containing specimens. For PLA and MBi series, the normalized analysis is shown in Fig. 7.

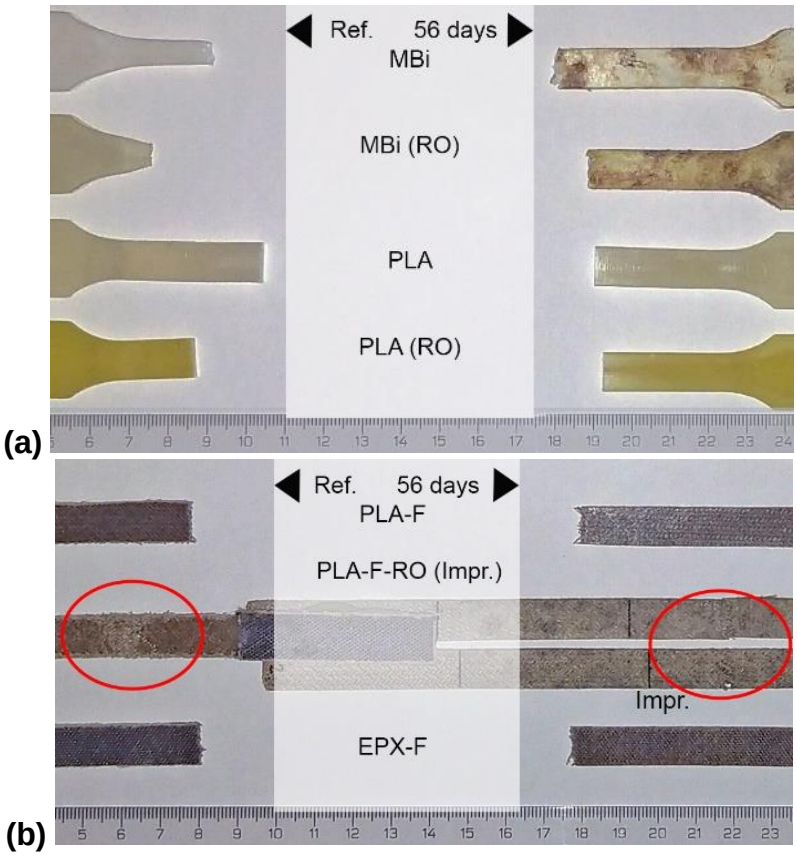

Fig. 4. Failure modes in tensile specimens shown for: a) reference specimens; and b) and specimens tested after 56 days of SB

The normalized effect of rosin on stiffness and modulus was calculated as the change in time (either 14 or 56 days) for non-RO-containing specimens and then, the change in time for RO-containing specimens was subtracted. When the change of stiffness and strength was larger for RO-containing specimens, the normalized value was negative, and RO was designated as having sped up the biodegradation. The normalized effects were analyzed with comparison to composite series in later sections. In summary, the PLA series was mechanically better performing with RO (due to higher stiffness with RO) and it was found to be more reasonable to study PLA with the flax reinforcement further.

Table 2. Effects of RO on the Mechanical Performance of Solid PLA and MBi and Degradation due to SB

Series	Young's Modulus (GPa)	Ultimate Engineering Strength (MPa)	Strain at Break (%)
PLA Ref. (0 days)	4.31 ± 0.77 *	61 ± 18 **	3.1 ± 1
PLA 14 days	2.37 ± 0.71	58 ± 17	4.7 ± 1
PLA 56 days	2.31 ± 0.53	57 ± 17	3.8 ± 1
PLA-RO Ref. (0 days)	4.90 ± 0.14 *	58.0 ± 16 **	3.2 ± 1
PLA-RO 14 days	2.14 ± 0.10	53.3 ± 15	6.7 ± 2
PLA-RO 56 days	2.04 ± 0.58	52.6 ± 15	5.6 ± 2
MBi Ref. (0 days)	0.169 ± 0.01 ***	9.5 ± 2 ****	79 ± 11
MBi 14 days	0.158 ± 0.01	9.6 ± 3	47 ± 9
MBi 56 days	0.162 ± 0.02	7.4 ± 3	12 ± 3
MBi-RO Ref. (0 days)	0.091 ± 0.01 ***	7.4 ± 3 ****	35 ± 11
MBi-RO 14 days	0.102 ± 0.01	6.8 ± 3	24 ± 9
MBi-RO 56 days	0.112 ± 0.01	5.9 ± 3	10 ± 3
* Difference in Young's modulus due to rosin +14%			
** Difference in strength due to rosin 0…-5%			
*** Difference in Young's modulus due to rosin -46% compared to the rosin-free series			
**** Difference in strength due to rosin -22% compared to the rosin-free series			

Crystallinity in PLA

In general, a high degree of crystallinity in PLA could lead to a low amount of degradability, as the oxygen and in general moisture permeability is low inside crystalline zones (Kyrikou and Briassoulis 2007). Therefore, the crystallinity in PLA series specimens was surveyed by using XRD first. There were no distinctive peaks to indicate significant crystallinity in the spectra (see spectra in the Appendix section). Also, there were no observable effects by the compounding of RO or SB (up to 56 days) on the spectra. The similarity in the XRD spectra (before SB) of PLA and PLA-RO series before composting is rather expected because they both went through similar melt-processing, *i.e.*, compounding and injection.

The DSC results, in Fig. 5, reveal that the degree of crystallinity (K) was low (4.6%) in pure PLA before SB and this result is in agreement with the XRD results. The SB conditioning did not significantly affect the degree of crystallinity (5.6%). The mixing of RO to PLA resulted in observably higher crystallinity (K = 11.8%) and the 14 days in SB did not decrease the crystallinity (K = 18.4%) of these blends. It should be noted that the crystallinity can locally vary in the injection-molded specimens and also the SB conditioning can affect the polymer in small local details. In terms of the mechanical properties, the increased crystallinity due to RO explains the Young's modulus being higher for PLA-RO compared to PLA (Table 2) and also the ultimate strength remained high.

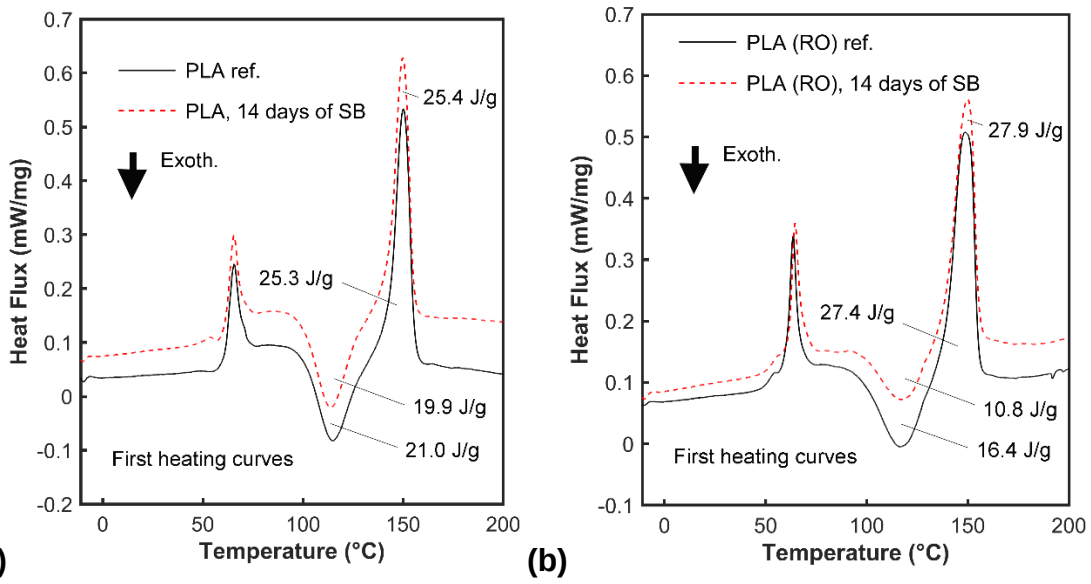

Fig. 5. DSC heat flux curves determined for: a) PLA; and b) PLA-RO in the reference state and after the soil burial of 14 days. The specimens were dried after soil burial before the measurements.

Mechanical performance of flax-reinforced PLA laminates

In this study, the free edges of the composite specimens were not sealed prior to SB. This was selected to represent the worst-case scenario – such as a broken device part, and to emphasize possible degradation effects of fiber-matrix interfaces and fibers themselves. Therefore, it was expected that all the composite specimens experienced fast degradation in terms of mechanical properties during SB compared to the non-reinforced, isotropic specimens.

Eventually, the RO-treated specimens over the course of the series in this study experienced a slightly higher mass loss after 56 days of SB: on average 0.37% higher mass loss compared to the specimens without any rosin content. However, this difference was primarily related to the composite laminates with flax reinforcement (*i.e.*, 0.46 to 0.50% higher mass loss). This higher amount of decomposition in flax-containing composites was anticipated to have occurred in the flax fibers themselves. Therefore, further analysis of the composites was necessary.

For the PLA-F and PLA-F-RO composites, the ultimate values of strength as well as the strain at break tend to stabilize after the 14 days of SB, as shown in Table 3 and Figs. 6 and 8. The failure modes of the PLA-F and EPX-F composite specimens were macroscopically brittle and localized, neat fractures, as shown in Fig 4b. The specimens with RO had the damage spread over a larger area so that some reinforcement was left continuous after ultimate failure (*i.e.*, the load dropped in practice to zero). Also, the stress-strain curves of these specimens (Figs. 6d and 6e) indicate gradual damage prior to peak stress – especially after 56 days of SB. The kinks in the stress-strain curves are linked to the wider spread of damage in the specimens. The series with RO-impregnated fibers experienced distinctively higher degradation after the first 14 days, as shown in Table 4.

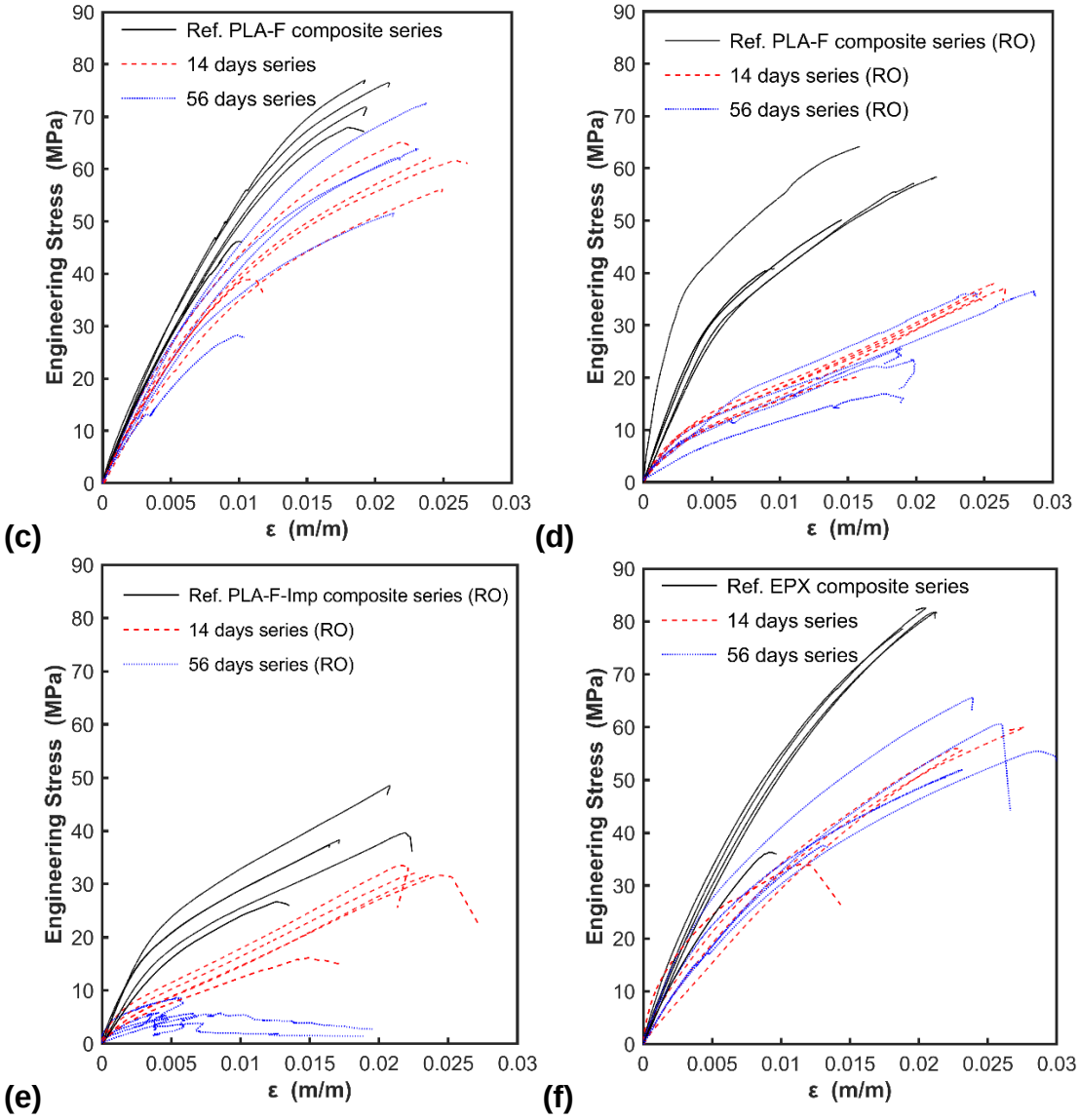

Fig. 6. Tensile stress-strain curves (c-d) of flax reinforced composites in the reference state and after the soil burial of 14 days and 56 days. The specimens were dried after soil burial before testing.

The way RO was used (impregnated or blended in) did have a distinct effect; the method of RO impregnation led to much greater degradation. The degradation of strength and modulus continued significantly after 14 days (Fig. 8) with impregnation, whereas it mostly stabilized for the RO-blended composites without impregnation (PLA-F-RO).

Because neither pure PLA nor PLA-RO series of the isotropic specimens showed strong continuation of degradation after 14 days of SB, the observed continuing degradation in the flax-containing PLA-F-Imp (Fig. 7, Table 4) must mostly occur: 1) inside the flax fibers, or 2) at the fiber-matrix interfaces. The effect of impregnation is in contradiction to what was originally expected and suggests continuing rupture at fiber-matrix interfaces after 14 days of SB. The rupture is probably due to moisture and hydrolysis because biotic (microbial) degradation is forecasted to decrease after the decrease in temperature of compost (Fig. 2). It should be noted that the RO-blended matrix (PLA-RO) was the same for the impregnated and non-impregnated composite specimens.

In Fig. 8, the relative stiffness and strength of the composites are given for 14 and 56 days of SB composting. The mechanical values are normalized by the values of specimens tested without any SB. Effects of RO cannot be normalized the same way as in Fig. 7 because the epoxy-flax composites did not contain any series with RO. It is important to note that the composite specimens had a non-unidirectional lay-up, and this means that the ultimate values of strength and modulus of the specimens greatly reflected the performance of matrix polymer and interfaces in addition to that of the fiber reinforcement. For unidirectional lay-ups in composites, the tensile test results would emphasize the performance of fibers.

Table 3. Effects of RO on the Mechanical Performance of PLA-F and EPX-F Composites and Degradation due to SB

Series	Young's Modulus (GPa)	Ultimate Engineering Strength (MPa)	Strain at Break (%)
PLA-F ref. (0 days)	5.75 ± 0.32 *	68 ± 21 **	1.8 ± 0.6
PLA-F 14 days	4.65 ± 0.32	57 ± 17	2.2 ± 0.7
PLA-F 56 days	4.51 ± 0.78	56 ± 18	2.0 ± 0.7
PLA-F-RO ref. (0 days)	6.35 ± 0.99 *	54 ± 16 **	1.6 ± 0.6
PLA-F-RO 14 days	2.25 ± 0.2	33 ± 9	2.3 ± 0.7
PLA-F-RO 56 days	1.93 ± 0.4	28 ± 10	2.2 ± 0.7
EPX-F ref. (0 days)	5.68 ± 0.64 ***	72 ± 24 ****	1.8 ± 0.6
EPX-F 14 days	3.71 ± 0.58 ***	41 ± 16 ****	1.8 ± 0.7
EPX-F 56 days	4.02 ± 0.76	54 ± 16	2.4 ± 0.7
* Difference in Young's modulus due to rosin +10% compared to the rosin-free series			
** Difference in strength due to rosin -20% compared to the rosin-free series			
*** Difference in Young's modulus due to 14 days of burial -35%			
**** Difference in strength due to 14 days of burial -43%			

The relative amount of degradation in the rival epoxy composites (EPX-F series) was essentially the same or even higher (see Table 3 and Fig. 8) when compared to the composites with PLA and PLA-RO matrices. However, the degradation process in terms of effects on strength and Young's modulus tended to cease after 14 days in the case of the epoxy composites. This dwell in the degradation process is anticipated due to the decreased compost temperature after the first 14 days, with potentially decreased diffusion of moisture into the epoxy-flax composites. Epoxy (resin) and epoxy-flax interfaces are relatively insensitive to decompose due to moisture at temperatures below the glass transition temperature (T_g). Thus, plasticization by diffused moisture and degradation of flax fibers are presumed to be the primary causes of degradation of EPX-F series specimens in this study.

Table 4. Effects of RO-impregnation on the Mechanical Performance of PLA-F Composites and Degradation

Series	Young's Modulus (GPa)	Ultimate Engineering Strength (MPa)	Strain at Break (%)
PLA-F-Imp-RO ref. (0 days)	5.11 ± 0.99 *	38 ± 11 **	1.8 ± 0.6
PLA-F-Imp-RO 14 days	2.2 ± 0.38	30 ± 9	2.2 ± 0.7
PLA-F-Imp-RO 56 days	1.14 ± 0.33	6 ± 9	1.1 ± 0.4
PLA-F-RO ref. (0 days)	6.35 ± 0.99 *	54 ± 16 **	1.6 ± 0.6
PLA-F-RO 14 days	2.25 ± 0.2	33 ± 9	2.3 ± 0.7
PLA-F-RO 56 days	1.93 ± 0.4	28 ± 10	2.2 ± 0.7
* Difference in Young's modulus due to the added impregnation treatment -19%			
** Difference in strength due to the added impregnation treatment -30%			

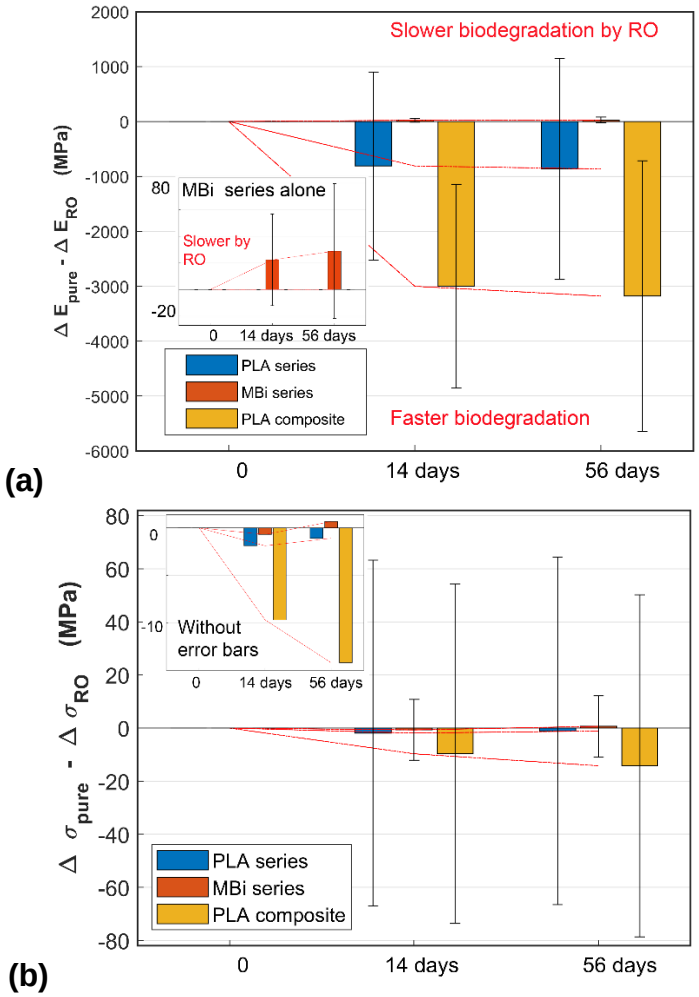

Fig. 7. The specific (faster or slower degradation) effect of RO per material on the change of mechanical properties in time: a) change in Young's modulus; b) change in maximum (peak) engineering stress. The PLA composite here refers to hot-pressed flax-reinforced laminate specimen, for the purpose of making a comparison to the unreinforced polymer series.

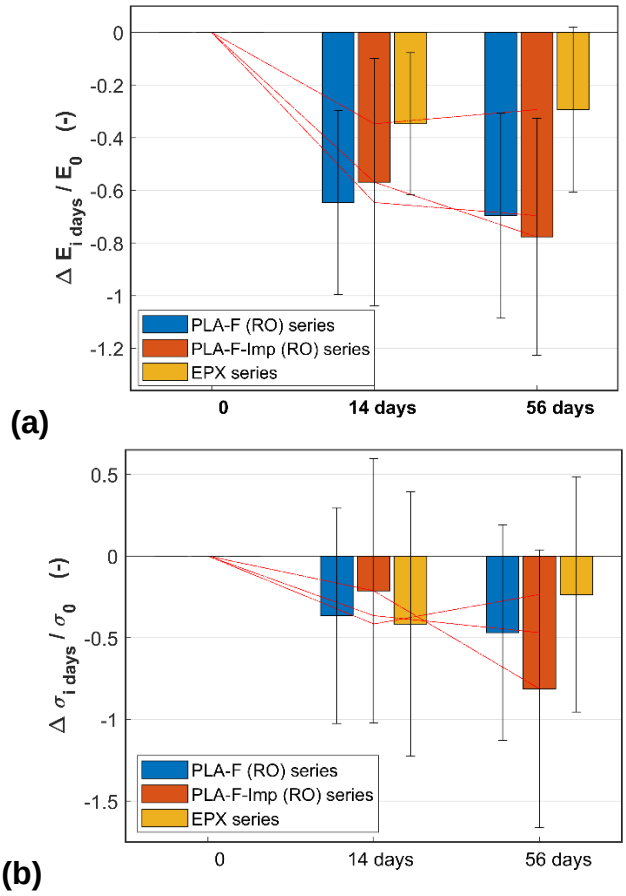

Fig. 8. The change (degradation) of mechanical performance of flax reinforced composite laminates with RO in terms of the relative change (per *i* days): a) Young's modulus; b) ultimate engineering stress. The epoxy-flax composite (EPX-F) does not have any rosin content and is shown for comparison.

Surface treatments of cellulose-containing reinforcements are considered to be compatibilizers (Hubbe *et al.* 2021) when increased adhesion *via* chemical bonds is reached. Impregnation of flax fibers with RO can lead to esterification by −COOH groups at hydroxyl-rich cellulosic fibers. In addition, for the impregnation process, the excess RO, inside (technical) fibers, is an antimicrobial substance that would be expected to partly block moisture diffusion in the reinforcement. However, the tensile test results clearly suggest stronger biodegradation in these composites with the RO-impregnated fibers. The effect of RO on fiber surfaces as a compatibilizer is considered in the next section with MB test results. When related to the role of fiber-matrix adhesion, an analysis of failure mode and interfacial adhesion was considered necessary to better understand fiber-matrix adhesion and its contribution to specific failure modes.

Failure Modes and Fiber-Polymer Interfacial Adhesion

Figure 9 shows the fracture surface of typical PLA-F composite specimens, and it shows an essentially void-less PLA matrix and clearly visible flax (technical) fibers. There are several signs of a mixed failure mode, including matrix cleavage and tearing, flax fiber pullout, and interfacial debonding. The details in Fig. 9b show that flax fibers experienced occasional adhesive failure but also maintained strong adherence to the surrounding PLA.

The failure modes in typical PLA-F-RO series specimens are shown in Fig. 10. The most distinctive change compared to the series without RO (*i.e.*, Fig. 9) is the larger number of voids. These voids contain both larger bubbles and small, pinhole-type voids near the flax fibers (Fig. 10b). The interfaces tend to perform similarly as in the series without RO; the failure amid the fibers involved some adhesive failure but also good adherence to the surrounding RO-blended PLA. The failure modes did not observably change due to SB (up to 56 days), as shown in Fig. 11. For example, signs of interfacial debonding did not increase due to SB.

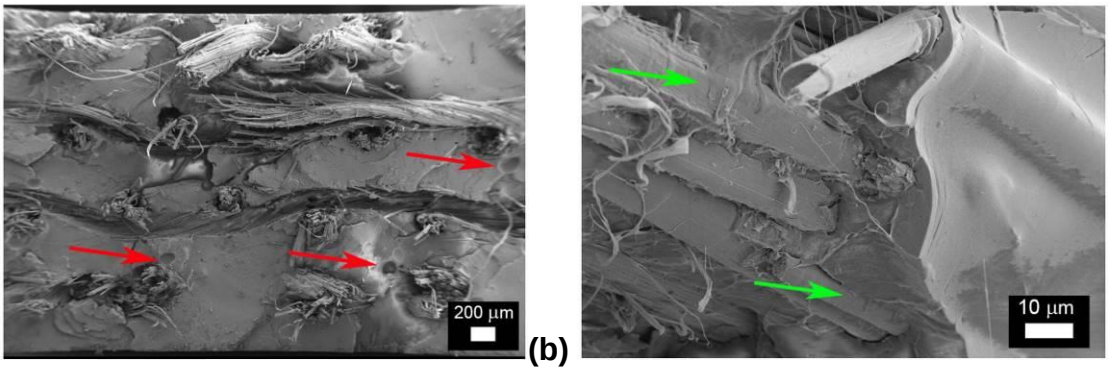

Fig. 9. Typical failure modes in tensile loaded flax reinforced PLA-F composites: a) general view; b) magnification towards fiber-matrix interfaces. Specimen condition here is as before SB (*i.e.*, the Ref. condition). The red arrows highlight micro-voids, and the green arrows highlight the adherence of fibers with the PLA matrix.

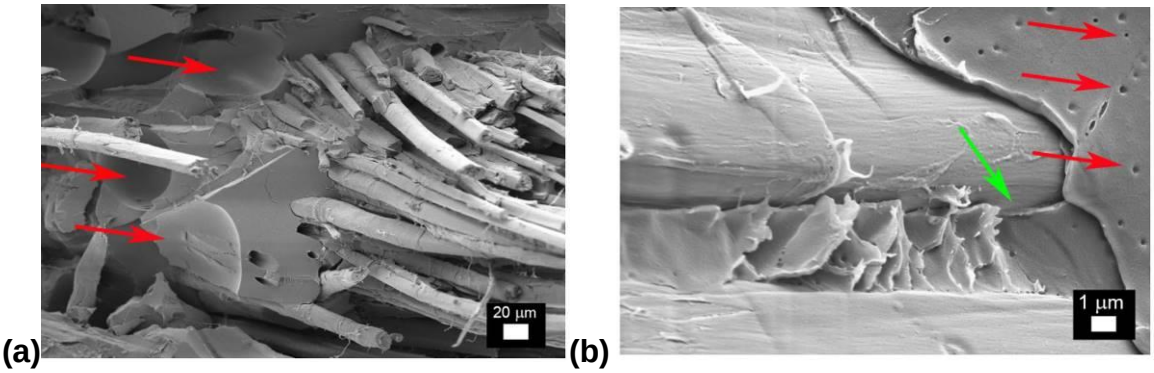

Fig. 10. Typical failure modes in tensile loaded flax reinforced PLA-F-RO composites: a) general view; b) magnification towards fiber-matrix interfaces. Specimen condition here is as before SB (*i.e.*, the Ref. condition). The red arrows highlight voids (in a) and pin holes (in b), and the green arrows highlight the adherence of fibers to the PLA matrix.

Because the interfacial performance at fracture surfaces of flax-containing PLA composites (PLA-F and PLA-F-RO series) indicated both adhesive and cohesive failure, more detailed testing and analysis was needed to understand the interfacial adhesion. Interface testing by using the MB method was performed to compare the effect of RO on micro-scale adhesion. Fig. 12a shows the results of MB testing.

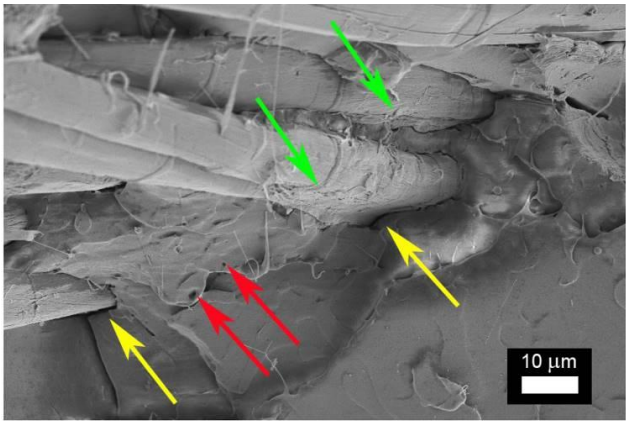

Fig. 11. Typical failure modes in tensile loaded flax reinforced PLA-F-RO composite after 56 days of SB. The red arrows highlight micro-voids, the green arrows highlight the adherence of fibers with the PLA matrix, and yellow arrows highlight local interfacial debonding.

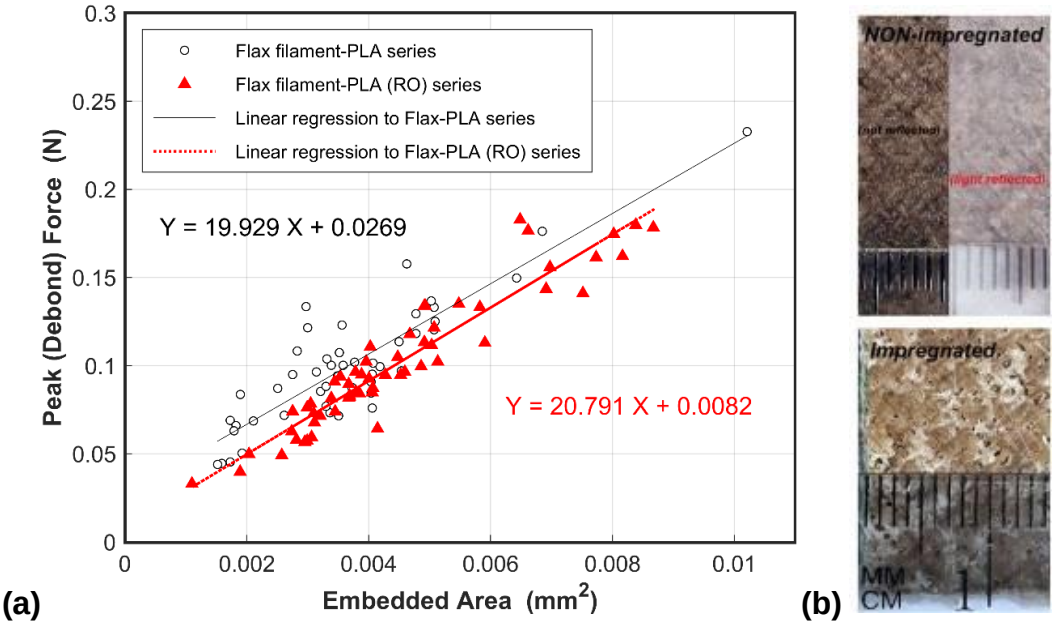

Fig. 12. a) MB test data for flax filaments with PLA droplets and flax filaments with and without impregnation by RO. b) Surface of PLA-F-RO and PLA-F-Imp-RO laminates after hot pressing

The interfacial debonding force (namely peak force) over a range of droplet sizes, in terms of the embedded area, was similar for the as-received flax fibers (*i.e.*, extracted filaments) and for the RO-treated filaments. The linear regressions of the data suggested a slightly higher slope for the RO-treated droplet samples. The slope is typically interpreted as the interfacial shear strength (IFSS) between the filament and the droplet polymer (herein PLA). Thus, RO did not decrease the adhesion of PLA to the pristine flax filaments in fresh, non-composted specimens of this study. Moreover, RO can be considered neutral in the sense of compatibilizer for increased chemical bonds between PLA and flax fibers. The effect of RO-impregnation on the moisture diffusion in composites during composting can still explain the large effect of impregnated fibers on the mechanical performance. The next section discusses the overall results and the effects of RO-impregnation on the preparation of specimens and the effects on moisture diffusion.

Discussion

In this study, rosin was shown to affect the mechanical degradation of both matrix polymers and composites with flax as a function of burial time. Typically, hydrolysis is expected to be the main decomposition reaction in biodegradable polymers. This especially applies to plastics that contain ester, lactose, or ketone groups (Müller 2014; Bastioli 2002). For microbial decomposition, the optimal conditions (for fungi) are approximately 70 to 90% RH, the temperature of 24 to 30 °C, and pH ≈6. Therefore, the degradation in this work is presumed to include both hydrolysis and microbial decomposition.

The rosin's effect on MBi series was interesting. In MBi, starch has been modified chemically into a practical polymer system (Müller 2014; Bastioli 2002). When compared to many traditional biodegradable polymers, MBi-like (starch-based) polymers suffer biodegradation even in household composting conditions (Czaja-Jagielska and Melski 2013). Although MBi is not considered for structural composites due to its low mechanics, it is a good candidate for many products. MBi is well able to degrade anaerobically (unlike PLA) (Massardier-Nageotte *et al.* 2006; Mohee *et al.* 2008), and the compounds released during biodegradation are not harmful to any of the bacteria in the soil (Sforzini *et al.* 2016). It should be noted that RO was observed to slow down biodegradation in terms of stiffness (and ultimate strength) in the MBi specimens of this study (Fig. 7a). This effect could perhaps be more pronounced for longer burial periods than 56 days.

PLA may decompose in soil, but the reaction is generally sensitive to the oxygen available and depending on the exact chemistry and crystallinity (poly (L-lactide), poly (DL-lactic acid), *etc*.) (Grizzi *et al.* 1995; Hakkarainen *et al.* 2000). For temperatures as in this study, PLA may not be very vulnerable to microbial attack (Tokiwa and Calabia 2006). This may be the reason why the rosin-blending caused faster degradation – the rosin itself may be decomposed by microbes in the moist soil. It has been indicated that rosin gets mixed as separate yet nano-sized phase in polymer blends (Kanerva *et al.* 2019). When rosins are mixed well, they are workable additives and do not decrease the performance of PLA.

The rosin-impregnated PLA composites of this study degraded especially during SB. Many fungi and bacteria (for example *Clostridium* and *Cytophaga* strains) can decompose natural fibers (Papaspyrides and Kiliaris 2013). In the current literature, natural fibers with cellulosic content have been observed to increase the biodegradation rate in PLA composites (Siakeng *et al.* 2019; Hubbe *et al.* 2021). Here, voids and pinholes were observed on the outer surfaces of the composite laminates right after the hot pressing of composites with impregnated fibers (see Fig. 11b). The melting temperature of PLA, required for the hot-pressing, clearly resulted in the formation of gaseous residues, anticipated due to the lightest molecular species in rosin or residual moisture left in the fibers. The voids or rows of voids in PLA presumably work as paths for moisture to emanate into the flax reinforcement. This diffusion is also fast in the event of rosin-blocked moisture diffusion inside the fibers themselves. The exact comparison of rosin-containing composites and rosin-free composites is challenging due to the different processing technique, the parameter values at least, that would be necessary for an equal preparation quality of composites. Moreover, cracks and voids could emerge in the process of biodegradation during composting according to the current literature (Melelli *et al.* 2021). In this study, it was not possible to identify an increase of voids or pin holes specifically during the SB. Therefore, the voids and pin-holes formed prior to burial were found to be the main reason for faster degradation in the composites with rosin-impregnated fibers.

The surface treatments of flax fibers for improved adhesion to thermoplastic matrix

polymers are urgently needed (Le Duigou *et al.* 2010; Saha *et al.* 2016; Siakeng *et al.* 2019). In this study, rosin-treated flax performed comparably with the as-received fibers. To develop the adjustment of a composite's biodegradation, the exact rosin composition should be studied, and the preparation of laminates should be optimized for quality. Gum rosin may contain residuals of sugars and other nutrients that certain bacteria and fungi are able to consume. This is the reason why specific rosins or rosin derivatives are needed to be studied. It should be noted that chemical derivatives of rosin or rosins of various plants (Vainio-Kaila *et al.* 2017b; Ekeberg *et al.* 2006) can lead to a different microbial response. In detail, carboxylic acid groups of different (acid) compounds may cause different enhancement (Hubbe *et al.* 2021) of biodegradation or abiotic degradation.

CONCLUSIONS

1. Rosin (RO) compounding with poly(lactic acid) (PLA) resulted in blends that had a higher Young's modulus (+14%), contrary to the blends where rosin was compounded with a starch polymer (MBi). Mechanical strength in the PLA-RO series remained essentially constant but got 22% lower in the MBi-RO series. For up to 56 days of soil burial studied, the rosin addition led to the following tendencies as a function of soil burial time: faster biodegradation in terms of strength (2.7% change in percentage degradation) of the PLA-based blends and, a slowing-down effect for the MBi-based blends (2.1% lesser degradation) in terms of strength.
2. Flax-reinforced composites with PLA suffered extensive biodegradation in terms of in-plane mechanical properties compared to the non-reinforced PLA-based blends. The degradation tended to stabilize after the first 14 days of burial except for the series with the RO-impregnated flax fibers. The relative changes in mechanical properties of the RO-blended composite materials, as a function of soil burial time, were comparable to the degradation in rival epoxy-matrix composites.
3. The hot pressing method used for consolidating flax reinforcement and PLA was concluded to result in partial thermal decomposition of rosin. This not only affected potential microbial response during elongated soil burial but created pinholes into the hot-pressed specimens. This effect of manufacture was especially noted in the case of RO-impregnated flax fibers.
4. The interfacial adhesion of PLA with RO-treated flax fibers remained on the same level as for flax fibers without RO treatment when analyzed with the microbond test data.

ACKNOWLEDGMENTS

This investigation received support from three different grants from Business Finland (9310/405, 9310/448, 1763/31/2016). Researchers P. Laurikainen and O. Orell are gratefully acknowledged for their contribution to the testing activities at Tampere University, Finland.

REFERENCES CITED

Abdel-Raouf, M., and Abdul-Raheim, A. (2018). "Rosin: Chemistry, derivatives, and applications: A review," *BAOJ Chemistry* 4(1), 039.

ASTM D 568-14 (2020). "Standard test method for tensile properties of plastics," ASTM International, West Conshohocken, PA.

Bastioli, C. (2002). "Starch -polymer composites," in: *Degradable Polymers,* G. Scott (ed.), Chapman & Hall, UK. DOI: 10.1007/978-94-017-1217-0_6

Bensadoun, F., Verpoest, I., Baets, J., Müssig, J., Graupner, N., and Davies, P. (2017). "Impregnated fibre bundle test for natural fibres used in composites," *Journal of Reinforced Plastic Composites* 136(1), 942-957. DOI: 10.1177/0731684417695461

Chapuisat, M., Oppliger, A., Magliano, P., and Christe, P. (2007). "Wood ants use resin to protect themselves against pathogens," *Proceedings of the Royal Society B: Biological Sciences* 274(1621), 2013-2017. DOI: 10.1098/rspb.2007.0531

Crawford, B., Pakpour, S., Kazemian, N., Klironomos, J., Stoeffler, K., Rho, D., Denault, J., and Milani, A. (2017). "Effect of fungal deterioration on physical and mechanical properties of hemp and flax natural fiber composites," *Materials* 10(11), 1252. DOI: 10.3390/ma10111252

Czaja-Jagielska, N., and Melski, K. (2013). "Biodegradation of starch-based films in conditions of nonindustrial composting" *Polish Journal of Environmental Studies* 22(4), 1039-1044.

Di Vito, D., Kanerva, M., Järveläinen, J., Laitinen, A., Pärnänen, T., Saari, K., Saari, K., Kukko, K., Hämmäinen, H., and Vuorinen, V. (2020). "Safe and sustainable design of composite smart poles for wireless technologies," *Applied Sciences* 10(1), article 7594. DOI: 10.3390/app10217594

Ekeberg, D., Flate, P., Eikenes, M., Fongen, M., and Naess-Andresen, C. (2006). "Qualitative and quantitative determination of extractives in heartwood of scots pine (*Pinus sylvestris* L.) by gas chromatography," *Journal of Chromatography A* 1109(2), 267-272. DOI: 10.1016/J.CHROMA.2006.01.027

Endres, H., and Sieber-Raths, A. (2011). "End-of-life options for biopolymers," in: *Engineering Biopolymers: Markets, Manufacturing, Properties and Applications,* Carl Hanser Fachbuchverlag, Germany.

Falkiewicz-Dulik, M., Janda, K., and Wypych, G. (2015). "Industrial biocides," in: *Handbook of Material Biodegradation, Biodeterioration, and Biostablization,* ChemTec Publishing, Earswick, Canada.

Fontanella, S., Bonhomme, S., Brusson, J., Pitteri, S., Samuel, G., Pichon, G., Lacoste, J., Fromageot, D., Lemaire, J., and Delort, A-M. (2013). "Comparison of biodegradability of various polypropylene films containing pro-oxidant additives based on Mn, Mn/Fe or Co", *Polymer Degradation and Stability* 98(4), 875-884. DOI: 10.1016/j.polymdegradstab.2013.01.002

Giancane, S., Panella, F., and Dattoma, V. (2010). "Characterization of fatigue damage in long fiber epoxy composite laminates," *International Journal of Fatigue* 32(1), 46-53. DOI: 10.1016/j.ijfatigue.2009.02.024

Graupner, N., Hohe, J., Schober, M., Rohrmüller, B., Weber, D., Bruns, L., Bruns, A., and Müssig, J. (2022). "A competitive study of the static and fatigue performance of flax, glass, and flax/glass hybrid composites on the structural example of a light railway axle tie," *Frontiers in Materials* 9, In Print. DOI: 10.3389/fmats.2022.837289

Grizzi, I., Garreau, H., Li, S., and Vert, M. (1995). "Hydrolytic degradation of devices

based on poly(DL-lactic acid) size-dependence," *Biomaterials* 16(4), 305-311. DOI: 10.1016/0142-9612(95)93258-F

Hakala, P., Javanshour, F., Jordan, J., Laaksonen, P., Jutila, L., Järveläinen, J., and Kanerva, M. (2022). "The performance of flax reinforced composites for wireless and sport applications: Natural additives and sandwich concepts," in: *Proceedings of the 20th European Conference on Composite Materials (ECCM)*, European Society for Composite Materials, Greece, in print.

Hakkarainen, M., Karlsson, S., and Albertsson, A. (2000). "Rapid (bio)degradation of polylactide by mixed culture of compost microorganisms—low molecular weight products and matrix changes," *Polymer* 41(1), 2331-2338. DOI: 10.1016/S0032-3861(99)00393-6

Himejima, M., Hobson, K., Otsuka, T., Wood, D., and Kubo, I. (1992). "Antimicrobial terpenes from oleoresin of ponderosa pine tree *Pinus ponderosa*: A defense mechanism against microbial invasion," *Journal of Chemical Ecology* 18(10), 1809-1818. DOI: 10.1007/BF02751105

Hoffmann, K., Haag, K., and Müssig, J. (2021). "Biomimetic approaches towards lightweight composite structures for car interior parts," *Materials and Design* 212, article 110281. DOI: 10.1016/j.matdes.2021.110281

Hubbe, M. A., Lavoine, N., Lucia, L. A., and Chang, D. (2021). "Formulating bioplastic composites for biodegradability, recycling, and performance: A review," *BioResources* 16(1), 2021-2083.

Imre, B., and Vilaplana, F. (2020). "Organocatalytic esterification of corn starches towards enhanced thermal stability and moisture resistance" *Green Chemistry* 22, 5017. DOI: 10.1039/d0gc00681e

Jutila, L. (2020). *The Re-design of a Sustainable Monocoque Shell for Ultra High Frequency Transmitting Radios*, Master's Thesis, Tampere University, Tampere, Finland, (http://urn.fi/URN:NBN:fi:tuni-202003192754), accessed 22 August 2022.

Kanerva, M., Puolakka, A., Takala, T., Elert, A., Mylläri, V., Jönkkäri, I., Sarlin, E., Seitsonen, J., Ruokolainen, J., Saris, P., and Vuorinen, J. (2019). "Antibacterial polymer fibres by rosin compounding and melt-spinning," *Materials Today Communications* 20, article 100527. DOI: 10.1016/j.mtcomm.2019.05.003

Kanerva, M., Matrenichev, V., Layek, R., Takala, T., Laurikainen, P., Sarlin, E., Elert, A., Yudin, V., Seitsonen, J., Ruokolainen, J., and Saris, P. (2020). "Comparison of rosin and propolis antimicrobials in cellulose acetate fibers against *Staphylococcus aureus*," *BioResources* 15(2), 3756-3773. DOI: 10.15376/biores.15.2.3756-3773

Kanerva, M., Mensah-Attipoe, J., Puolakka, A., Takala, T., Hyttinen, M., Layek, R., Palola, S., Yudin, V., Pasanen, P., and Saris, P. (2021). "Weathering of antibacterial melt-spun polyfilaments modified by pine rosin," *Molecules* 26(4), article 876. DOI: 10.3390/molecules26040876

Kumar, R., and Kumar, S. (2012). "Properties of plastics and composites prepared from different sources/grades of PLA," in: *Polylactic Acid: Synthesis, Properties, and Applications*, V. Piemonte (ed.), Nova Science Publishers, NY, USA.

Kumar, R., Yakubu, K., and Anandjiwala, R. (2010). "Biodegradation of flax fiber reinforced poly lactic acid," *Express Polymer Letters* 4(7), 423-430. DOI: 10.3144/expresspolymlett.2010.53

Kyrikou, I., and Briassoulis, D. (2007). "Biodegradation of agricultural plastic films: A critical review," *Journal of Polymers and the Environment* 15(2), 125-150. DOI: 10.1007/s10924-007-0053-8

Laurikainen, P., Kakkonen, M., von Essen, M., Tanhuanpää, O., Kallio, P., and Sarlin, E. (2020). "Identification and compensation of error sources in the microbond test utilising a reliable high-throughput device," *Composites Part A: Applied Sciences and Manufacturing* 137(1), article 105988. DOI: 10.1016/j.compositesa.2020.105988

Le Duigou, A., Davies, P., and Baley, C. (2010). "Interfacial bonding of flax fibre/poly(l-lactide) bio-composites," *Composites Science and Technology* 70(2), 231-239. DOI: 10.1016/j.compscitech.2009.10.009

Massardier-Nageotte, V., Pestre, C., Cruard-Pradet, T., and Bayard, R. (2006). "Aerobic and anaerobic biodegradability of polymer films and physico-chemical characterization," *Polymer Degradation and Stability* 91(3), 620-627. DOI: 10.1016/j.polymdegradstab.2005.02.029

Melelli, A., Pantaloni, D., Balnois, E., Arnould, O., Jamme, F., Baley, C., Beaugrand, J., Shah, D., and Bourmaud, A. (2021). "Investigations by AFM of ageing mechanisms in PLA-flax fibre composites during garden composting," *Polymers* 13(14). DOI: 10.3390/polym13142225

Mohee, R., Unmar, G., Mudhoo, A., and Khadoo, P. (2008). "Biodegradability of bio-degradable/degradable plastic materials under aerobic and anaerobic conditions," *Waste Management* 28(9), 1624-1629. DOI: 10.1016/j.wasman.2007.07.003

Müller, R-J. (2014). "Biodegradation behaviour of polymers in liquid environments" in: *Handbook of Biodegradable Polymers*, C. Bastioli (ed.), Smithers Rapra, UK.

Niu, X., Liu, Y., Song, Y., Han, J., and Pan, H. (2018). "Rosin modified cellulose nanofiber as a reinforcing and co-antimicrobial agents in polylactic acid/chitosan composite film for food packaging," *Carbohydrate Polymers* 183, 102-109. DOI: 10.1016/j.carbpol.2017.11.079

Ojeda, T., Freitas, A., Dalmolin, E., Pizzol, M., Vignol, L., Melnik, J., Jacques, R., Bento, F., and Camargo, F. (2009). "Abiotic and biotic degradation of oxo-biodegradable foamed polystyrene," *Polymer Degradation and Stability* 94(12), 2128-2133. DOI: 10.1016/j.polymdegradstab.2009.09.012

Oliveux, G., Dandy, L., and Leeke, G. (2015). "Current status of recycling of fibre reinforced polymers: Review of technologies, reuse and resulting properties," *Progress in Materials Science* 72(1), 61-99. DOI: 10.1016/j.pmatsci.2015.01.004

Papaspyrides, C., and Kiliaris, P. (2013). in: *Polymer Green Flame Retardants*, Elsevier Science, The Netherlands.

Puchalski, M., Kwolek, S., Szparaga, G., Chrzanowski, M., and Krucinska, I. (2017). "Investigation of the influence of PLA molecular structure on the crystalline forms (α' and α) and mechanical properties of wet spinning fibres," *Polymers* 9(1), 18. DOI: 10.3390/polym9010018

Ray, S. S., and Okamoto, M. (2003). "Biodegradable polylactide and its nanocomposites: opening a new dimension for plastics and composites," *Macromolecular Rapid Communications* 24(14), 815-840. DOI: 10.1002/marc.200300008

Rudnik, E. (2008). "Composting methods and legislation," in: *Compostable polymer materials*, Elsevier Science, UK.

Saha, P., Chowdhury, A., Roy, D., Adhikare, B., Kim, J., and Thomas, S. (2016). "A brief review on the chemical modifications of lignocellulosic fibers for durable engineering composites," *Polymer Bulletin* 73(2), 587-620. DOI: 10.1007/s00289-015-1489-y

Sforzini, S., Oliveri, L., Chinaglia, S., and Viarengo, A. (2016). "Application of biotests for the determination of soil ecotoxicity after exposure to biodegradable plastics," *Frontiers in Environmental Science* 4, 68. DOI: 10.3389/fenvs.2016.00068

Siakeng, R., Jawaid, M., Ariffin, H., Sapuan, S., Asim, M., and Saba, N. (2019). "Natural fiber reinforced polylactic acid composites: A review," *Polymer Composites* 40(2), 446-463. DOI: 10.1002/pc.24747

Singh, R. P., Pandey, J. K., Rutat, D., Degée, P., and Dubois, P. (2003). "Biodegradation of poly(ε-caprolactone/starch blends and composites in composting and culture environments: the effect of compatibilization on the inherent biodegradability of the host polymer," *Carbohydrate Research* 338(17), 1759-1769. DOI: 10.1016/S0008-6215(03)00236-2

Sjöström, E. (1993). "Extractives" in: *Wood Chemistry - Fundamentals and Applications*, Academic press, Massachusetts, USA.

Skakovskii, E., Tychinskaya, L., Gaidukevich, O., Kozlov, N., Klyuev, A., Lamotkin, S., Shpak, S., and Rykov, A. (2008). "NMR determination of the composition of balsams from Scotch pine resin," *Journal Appl Spectroscopy* 75(3), 439-443. DOI: 10.1007/s10812-008-9065-y

Söderberg, T., Gref, R., Holm, S., Elmros, T., and Hallmans, G. (1990). "Antibacterial activity of rosin and resin acids in vitro," *Scandinavian J Plastic & Reconstructive Surgery & Hand Surgery* 24(3), 199-205. DOI: 10.3109/02844319009041279

Tokiwa, Y., and Calabia, B. (2006). "Biodegradability and biodegradation of poly(lactide)," *Applied Microbiology and Biotechnology* 72(2), 244-251. DOI: 10.1007/s00253-006-0488-1

Vainio-Kaila, T., Hänninen, T., and Kyyhkynen, A. (2017a). "Effect of volatile organic compounds from *Pinus sylvestris* and *Picea abies* on *Staphylococcus aureus*, *Escherichia coli*, *Streptococcus pneumoniae* and *Salmonella enterica* serovar Typhimurium," *Holzforschung* 71, 905-912. DOI: 10.1515/hf-2017-0007

Vainio-Kaila, T., Zhang, X., Hänninen, T., Kyyhkynen, A., Johansson, L., Willför, S., Österberg, M., Siitonen, A., and Rautkari, L. (2017b). "Antibacterial effects of wood structural components and extractives from *Pinus sylvestris* and *Picea abies* on Methicillin-resistant *Staphylococcus aureus* and *Escherichia coli* o157:h7," *Bioresources* 12(4), 7601-7614. DOI: 10.15376/biores.12.4.7601-7614

Veshagh, A., Marval, S., and Woolman, T. (2012). "Making the business case for eco-design and sustainable manufacturing," in: *Proceedings of the 19th CIRP Conference on Life Cycle Engineering*, Springer, Germany, pp. 11-17.

Yazdanbakhsh, A., and Bank, L. (2014). "A critical review of research on reuse of mechanically recycled FRP production and end-of-life waste for construction," *Polymers* 6(6), 1810-1826. DOI: 10.3390/polym6061810

Article submitted: August 26, 2022; Peer review completed: September 24, 2022; Revised version received and accepted: November 18, 2022; Published: December 6, 2022.
DOI: 10.15376/biores.18.1.899-925

APPENDIX

Supplemental Material

Additional SB-related data

The contents of the activators added into the compost soil are given Table A1.

Table S1. Contents in the Compost Activators as Provided by Manufacturers

Producer	Bacteria	Enzymes	Other, Fungi
Multikraft	*Lacticaseibacillus casei, Lactobacillus plantarum, Rhodopseudomonas palustris*	(none)	Yeasts (*Saccharomyces cerevisiae*)
Oy Neko AB	strains of *Bacillus* and *Pseudomonas* genus	unspecified enzymes	Fungi of *Aspergillus* and *Trichoderma* genus

MS and NMR spectra of rosin

The mass spectrometry (MS) and NMR spectra measured for the rosin in this study are shown in Fig. S1. In general, the (NMR) spectra of rosins were quite complicated due to the presence of a mixture of resin acids, such as dehydroabietic acid, abietic acid, isomers of abietic acid, and their methyl esters. The doublet peaks in the aromatic region at 7.172 ppm (J = 8.02 Hz) and 7.004 ppm (J = 8.02 Hz) and the singlet peak at 6.885 ppm indicate the presence of dehydroabietic acid. The presence of a peak at 6.201 ppm for olefinic hydrogen indicate the presence of neoabietic acid. Abeitic acid in the mixture could be confirmed from the peaks at 5.775 ppm and 5.380 ppm. The presence of pimaric acid in rosin could be confirmed from the peaks at 5.748 ppm, 5.143 ppm, 4.966 ppm, and 4.930 ppm. Isopimaric acid could be confirmed by the presence of peaks at 5.847 ppm, 5.334 ppm, 4.945 ppm, and 4.896 ppm. Levopimaric acid's presence in rosin could be identified from the peaks at 5.534 ppm and 5.143 ppm. The olefinic hydrogen at 5.390 ppm indicate the presence of palustric acid. Due to the overlapping of the signals in the aliphatic region of the spectrum, the discussion of this region is avoided for convenience.

a)

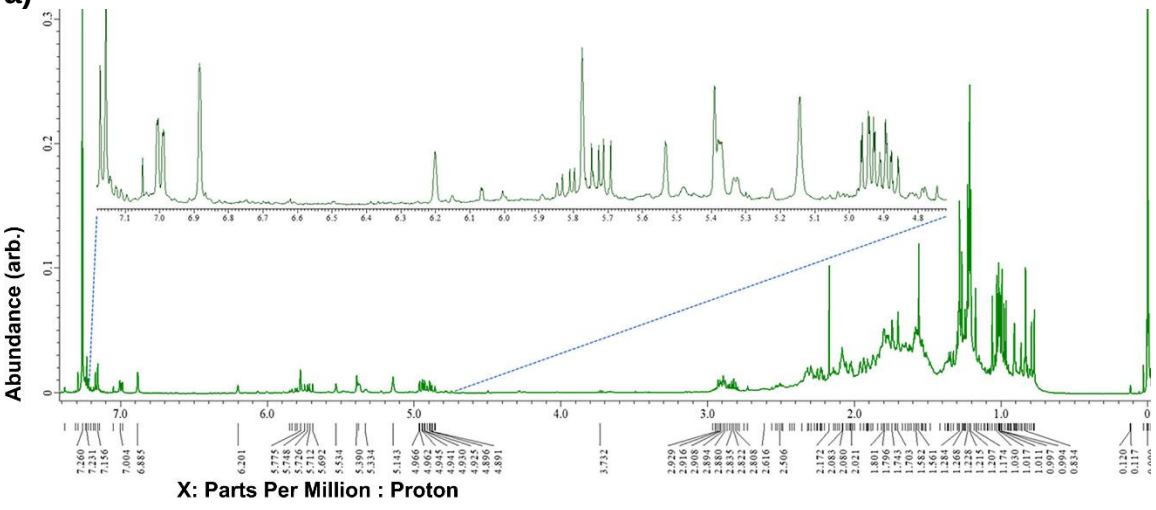

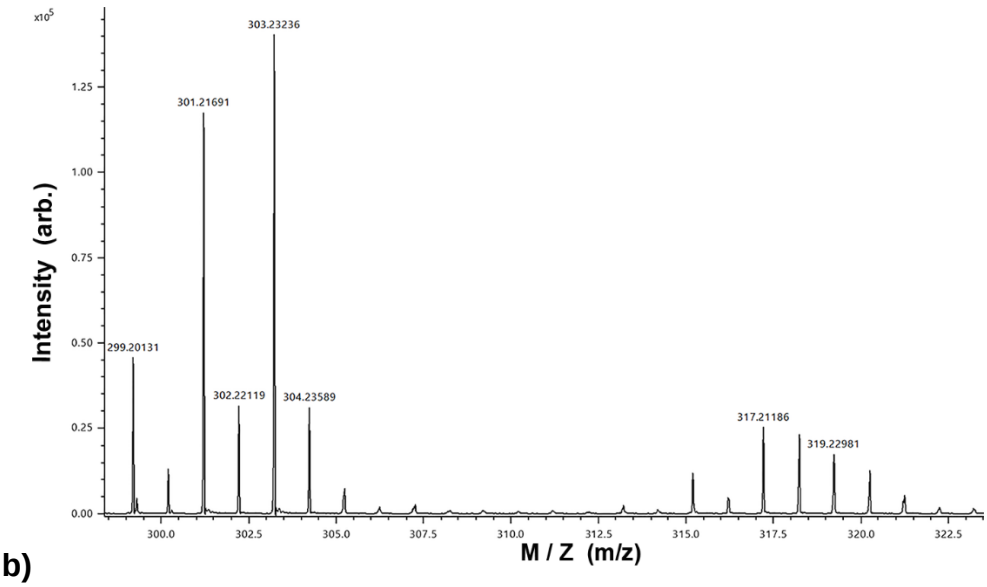

Fig. S1. a) MS spectrum of the rosin sample in this study. b) NMR proton spectrum of the rosin sample in this study.

XRD spectra of PLA

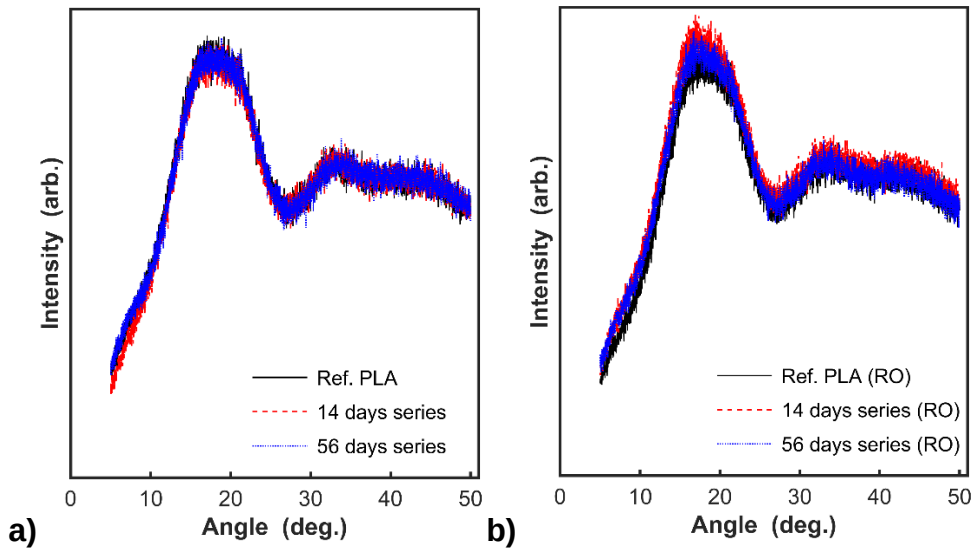

Fig. S2. XRD spectra of a) pure PLA in the reference condition and after SB of 14 and 56 days; b) PLA-RO in reference condition and after SB of 14 and 56 days

Additional mechanical data

The stress-strain behavior of MBi and MBi-RO blends in terms of true stress and logarithmic strain ($\varepsilon=\varepsilon_{lg}$) are shown in Fig. S3.

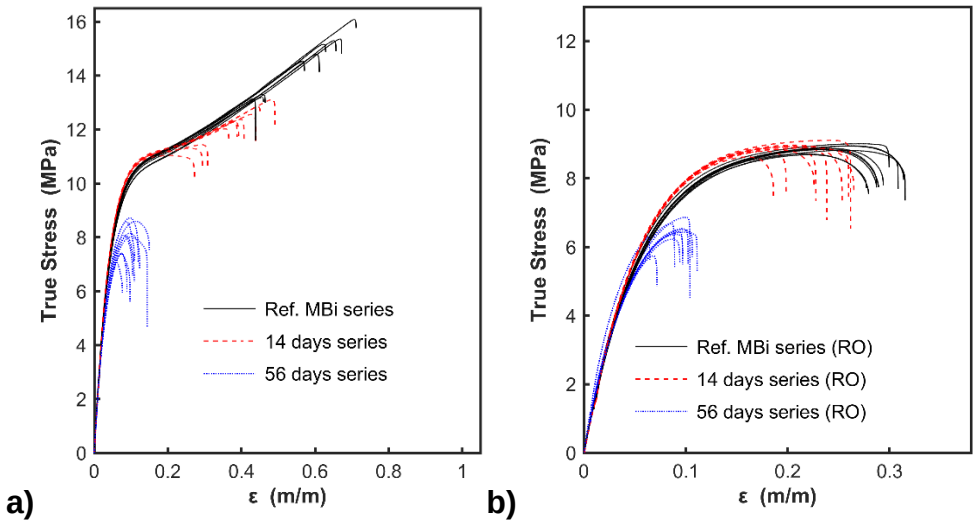

Fig. S3. Tensile true stress-strain curves for MBi blends in the reference state and after SB of 14 days and 56 days. The specimens were dried after SB before testing.